WPPFC-CPR(17) 18490

R Stadlmayr et al.

# Fluence dependent changes of surface morphology and sputtering yield of iron: comparison of experiments with SDTrimSP-2D

Preprint of Paper to be submitted for publication in Proceeding of
22nd International Workshop on Inelastic Ion-Surface Collisions

This work has been carried out within the framework of the EUROfusion Consortium and has received funding from the Euratom research and training programme 2014-2018 under grant agreement No 633053. The views and opinions expressed herein do not necessarily reflect those of the European Commission.

# Fluence dependent changes of surface morphology and sputtering yield of iron: comparison of experiments with SDTrimSP-2D

R. Stadlmayr[a,*], P.S. Szabo[a], B.M. Berger[a], C. Cupak[a], R. Chiba[a #], D. Blöch[a], D. Mayer[a], B. Stechauner[a], M. Sauer[b], A. Foelske-Schmitz[b], M. Oberkofler[c], T. Schwarz-Selinger[c], A. Mutzke[d], and F. Aumayr[a]

[a] *Inst. of Applied Physics, TU Wien, Fusion@ÖAW, Wiedner Hauptstraße 8-10, 1040 Vienna, Austria*

[b] *Analytical Instrumentation Center, TU Wien, 1060 Vienna, Austria*

[c] *Max-Planck-Institut für Plasmaphysik, Bolzmannstraße 2, 85748 Garching, Germany*

[d] *Max-Planck-Institut für Plasmaphysik, Wendelsteinstraße 1, 17491 Greifswald, Germany*

## Abstract

The influence of surface morphology modifications on the sputtering of thin Fe films by monoenergetic Ar ions is studied by using a highly sensitive quartz crystal microbalance technique. The morphology changes are induced by prolonged sputtering up to a total fluence of ≈ 7 x $10^{21}$ ions/m$^2$. Atomic force microscopy (AFM) measurements are performed to analyse the sample topography before and after irradiation and to evaluate surface roughness parameters. Numerical modelling with the codes SDTrimSP and SDTrimSP-2D are performed for comparison. Our investigations show that by using the local distribution of projectile impact angles, as derived from AFM measurements, as well as the elemental composition of the samples as an input to the codes SDTrimSP and SDTrimSP-2D the agreement between measurement and simulations is substantially improved.

*Keywords: Sputtering, Erosion, Quartz-crystal-microbalance, Surface Roughness, Trim*

*Corresponding author Reinhard Stadlmayr, e-mail: stadlmayr@iap.tuwien.ac.at

#present address: Tokyo Institute of Technology, Meguro-ku, Tokyo, 152-8550 Japan

## 1. Introduction

Ion induced sputtering is still one of the most important topics of ion-surface interaction and has a wide variety of practical applications, like surface etching, thin-layer deposition or surface analytic techniques. Sputtering also plays a major role in erosion of wall material in nuclear fusion devices [1] or in space weathering effects observed on lunar or planetary surfaces by solar wind ion impact [2, 3]. Plasma facing components (PFC) in a fusion device are constantly eroded by ion and neutral particle bombardment, which limits their lifetime. For a future fusion power plant tungsten is foreseen as material for PFCs and tungsten containing steels, like EUROFER are considered as possible alternatives for recessed areas in the reactor vessel [4]. Experiments with Fe-W sample films (with 1.5 at% W), which can be seen as a model system for EUROFER, showed a significant reduction of the erosion rate during low energy ion bombardment. The reduced erosion rate was explained by preferential sputtering of Fe, causing a W surface enrichment [5]. However modifications of the surface structure due to erosion were measured in addition [6], especially at steep angle of incidence, which also influence the sputtering behaviour. In order to separate the effect of surface enrichment of high Z materials from the effect of surface structural modifications, we set out to conduct sputtering experiments with pure Fe sample films and investigated the effect of surface morphology changes on the sputtering yield due to prolonged ion erosion.

Theoretical descriptions (e.g. [7]) and simulations (e.g. [8]) of sputtering often only take into account perfectly flat surfaces. However, this is an idealization, and while it is possible to create reasonably flat films for some materials, this assumption will lead to discrepancies with the actual experimental conditions. Figure 1 shows a sketch of how the roughness of a surface may affect the sputtering process. It shows a projectile ion hitting the surface under a nominal angle of 0 degrees, which would mean normal incidence for a perfectly flat surface. However, due to the rough surface condition the local angle of incidence $\theta$ is different, with its value being strongly dependent on the exact point of incidence. There, beside surface sputtering also projectile reflection may occur. On average $Y(\theta)$ (sputtering yield as a function of local impact angle) atoms are sputtered preferentially in the direction of the local surface normal per incident projectile. As is indicated in figure 1, not all of the sputtered atoms are able to escape the surface. Some of them may hit other parts of the rough surface and are deposited there. Additionally, the projectile is reflected with a certain probability and may hit the surface a second time. The energy of the reflected projectile is lower than the incident energy, but might still be high enough to lead to further sputtering. These sputtered particles are then again partly redeposited (omitted in figure 1 for clarity) and with a given probability further reflection may occur.

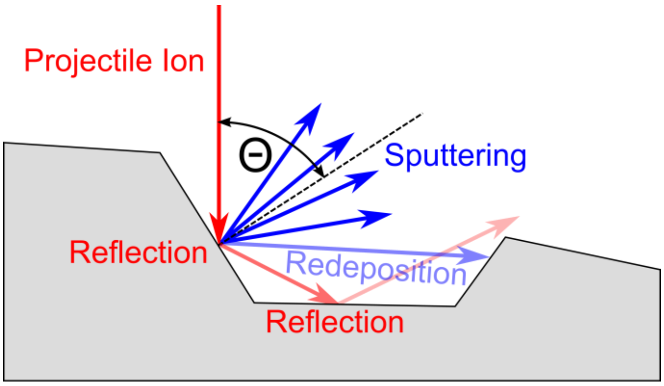


**Figure 1:** Sputtering of a rough surface. A projectile ion, which is represented by the red arrow, hits a surface under nominal normal incidence. The local angle of incidence θ differs, however, due to the surface structure and thus affects the sputtering yield. Some of the sputtered atoms cannot escape the surface and get redeposited, while multiple reflections of the projectile ion may lead to further erosion of the surface (after [9]).

Evidently, a theoretical description of the sputtering of rough surfaces becomes quite complex. Küstner et al. achieved remarkable results using STM images as an input and a simple model to describe redeposition effects ([9, 10]). However, more detailed modelling of this situation is necessary to take into account effects such as shadowing (especially for flat ion incidence, some parts of the surface will not be accessible by ions) and the change in angular and energy distributions, where figure 1 already indicates large changes compared to a flat surface. For this reason, we have used the newly developed SDTrimSP-2D code [11, 12] to take the actual surface structure into account in the sputtering simulations and compare the results of the simulations to our experimental data.

## 2. Experimental Approach

The measurements have been performed using a highly sensitive quartz crystal microbalance (QCM) developed at TU Wien and described in more detail in [13, 14]. This setup is an ideal tool to measure small mass changes and allows in-situ investigation of a dynamic erosion behaviour [6, 15]. Our investigations concentrated on mono-energetic Ar ions of 500 eV hitting an Fe-coated QCM sample. Ar might be used as seeding gas in fusion reactors like ITER, to avoid local overheating of the PFCs by radiative cooling [16]. Additionally Ar -> Fe sputtering yields are significantly higher than D –> Fe sputtering yields, making $Ar^+$ projectiles ideally suited for our experiments.

Typically 400 nm thin Fe films were deposited onto polished quartz crystals, by using a magnetron sputter deposition technique at IPP Garching, Germany. As the QCM technique only allows the measurement of the total mass change of the quartz and the presence of an oxide layer on the Fe film was assumed, one of the Fe films was analysed by X-Ray Photoelectron Spectroscopy (XPS). A sputter XPS system at the Analytical Instrumentation Center of TU Wien was used to obtain the quantitative elementary analysis as a function of depth.

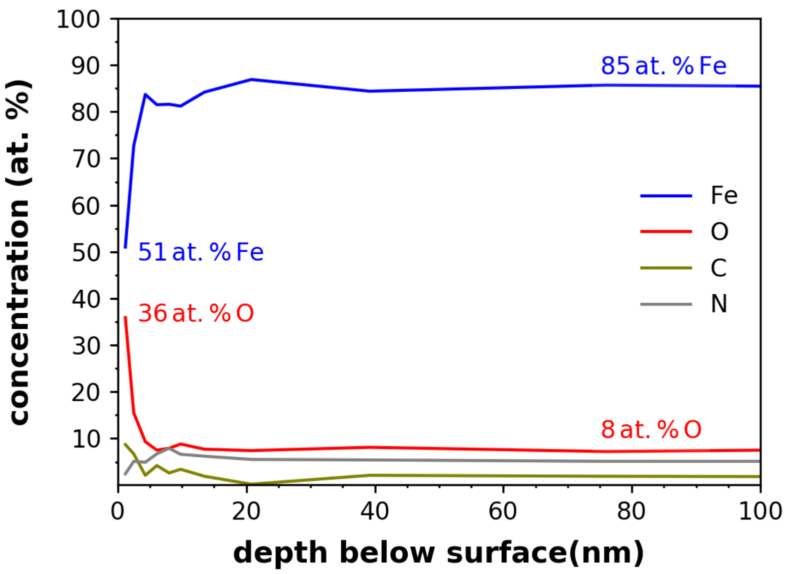


**Figure 2:** The XPS analysis of the Fe-film as function of depths shows a significant oxide layer on top of the sample. However, due to substantial O, N and C impurities even in the bulk the Fe concentration only reaches about 85%.

XPS results are given in figure 2 and show a high concentration of O at the surface indicating a native oxide layer as expected. Surprisingly, however, even in the bulk the Fe concentration only reaches 85% with substantial concentrations of O, N and C. We will show below, that for the simulations it is essential to take the actual elemental composition into account.

The evolution of the sputtering behaviour of the Fe model films under Ar ion bombardment was then investigated at the specific angle of incidence of α = 60° and in dependence of the bombarding ion fluence (results are shown in section 4). Measurements were performed at an ion flux of ≈ 5 x $10^{16}$ Ar/$m^2$ and a base pressure of 1 x $10^{-7}$ mbar.

AFM images of the Fe-coated QCMs were taken before and after prolonged irradiation (see fig. 3a and b). On the initial surface, grain-like features are visible (fig. 3a) that significantly change during the ion bombardment. For example after application of a total fluence of 6.7 x $10^{21}$ Ar/$m^2$ under an angle of incidence of 60° a ripple-like structure strongly aligned with the incoming projectile direction becomes visible (fig. 3b).

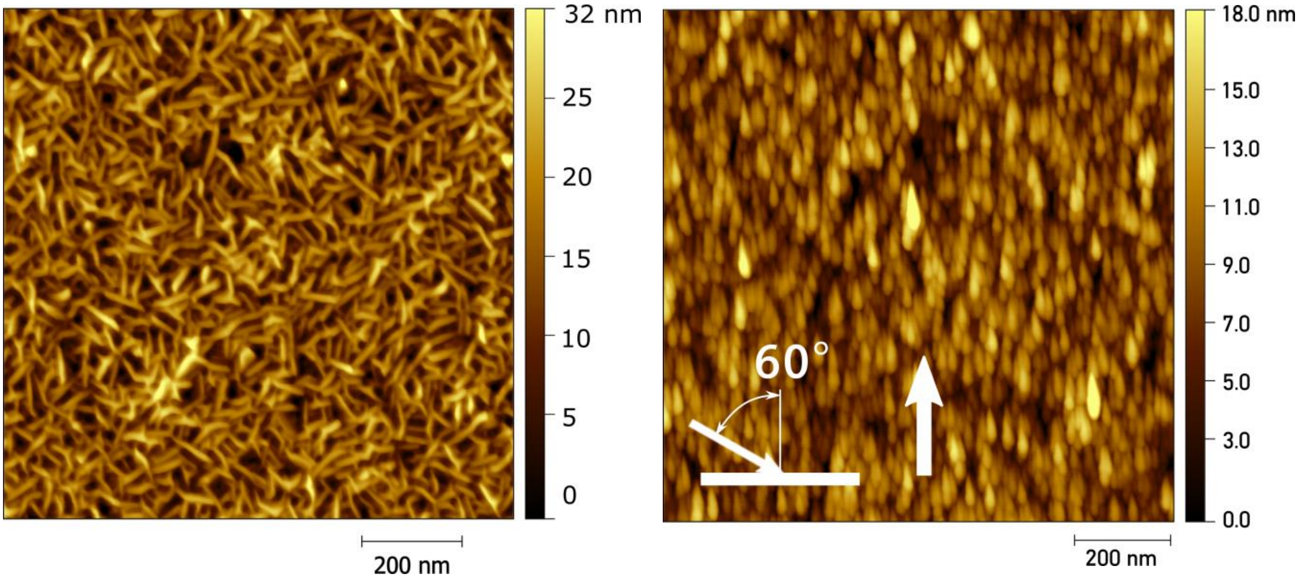


(a) (b)

**Figure 3:** AFM images of the target before **(a)** and after **(b)** ion irradiation with a total fluence of 6.7 x $10^{21}$Ar/$m^2$ show a significant change of the surface structure. Grain-like features that can be observed on an unirradiated sample transform into ripple-like structures [17], which are clearly aligned with the direction of irradiation (indicated by the white arrow).

## 3. Modelling with SDTrimSP

SDTrimSP is a Monte Carlo code that allows the simulation of ions hitting a solid target based on the binary collision approximation (BCA) [12, 18]. It represents a dynamic enhancement of the widely used "static" SRIM code [19] and the dynamic code TRIDYN [20, 21]. SDTrimSP results perform very well for calculating sputtering yields especially compared to the SRIM code [22]. The target in a SDTrimSP calculation is set up one-dimensionally, where several discrete layers of different compositions can be defined. This means that only depth-dependent aspects of the target's change due to particle bombardment can be taken into account.

The two-dimensional expansion SDTrimSP-2D developed at the Max Planck Institute of Plasma Physics (IPP) allows implementing a surface structure into an SDTrimSP simulation [11]. This is realized by expanding the geometrical description from layers to a grid, where the cell modification is calculated from the material transport following the collision cascades. Surface cells can grow and shrink based on the transport of target atoms and thus a change in the surface morphology can be simulated. First results presented in [23] were rather promising and reproduce experimental observations precisely.

The surface topography of our Fe films as deduced from the AFM measurements (fig. 3) was used as an input for SDTrimSP-2D. However, the AFM images in figure 3 clearly show a structure that cannot easily be reduced to two dimensions without omitting important information about the surface. Taking one line of (x, z)-coordinates of the AFM image would, for example, result in a surface that would appear much flatter because any additional inclination in y-direction would be ignored. For this reason an initial 2D target was created which has the same RMS roughness value as the real sample and the same distribution of the "local impact angles θ" (cf. section 4). This distribution shows the range of impact angles between the local surface normal and projectile incidence direction (see fig. 1). A target consisting of 10 initial layers with different concentrations of Fe, C, N and O according to the elemental composition retrieved from the XPS analysis (see fig. 2) was created. The final target surface that was used as a starting point for the SDTrimSP-2D simulations is shown in fig. 6a, with the color scale in this figure denoting the O concentration.

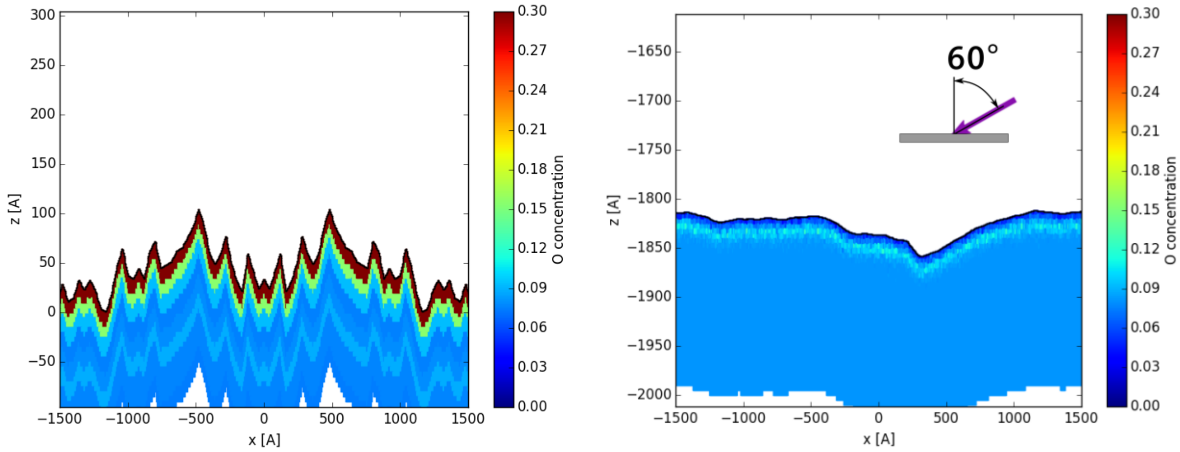


(a) (b)

**Figure 4: (a)** The model surface used as input for the SDTrimSP-2D simulations. The color represents the O concentration in the respective area. The surface was created to have the same distribution of local impact angles and RMS value as the one derived from the AFM image in fig. 3a. **(b)** After irradiation with 500 eV Ar ions up to a total fluence of 6.5 x $10^{21}$ Ar/m$^2$ impinging under a nominal angle of incidence of 60° from the right, the simulations show a smoothening of the surface consistent with the experimental data presented in fig. 5. Additionally an oxide depletion at the surface occurs.

Using this model target, SDTrimSP-2D simulations with 500 eV Ar were performed. On the one hand, the fluence dependence of the sputtering yield as well as the change of the surface morphology during the irradiation was simulated. On the other hand, the angular dependence of the sputtering yield before and after these irradiations was investigated. The results of these simulations are presented in the following section along and compared to the experimental data.

## 4. Comparison of experimental results to SDTrimSP-1D and SDTrimSP-2D

Figure 5 shows the measured fluence dependent sputtering yield of the Fe coated QCM sample when irradiated by 500eV Ar ions at an angle of incidence of 60 degree. The sputtering yield increases from 0.8 Fe/Ar to 1.9 Fe/Ar and reaches steady state after a fluence of about 2-3 x $10^{21}$ Ar/m$^2$. The observed initial strong change of the sputtering yield is due to the removal of an oxide layer, while changes at higher fluences indicate the change in surface morphology/roughness. The SDTrimSP-1D simulation assuming a target with pure Fe shows no fluence dependence and a constant sputtering yield of 2.2 Fe/Ar, which is higher than the actual measurements. A detailed analysis of our simulation results show that the main reason for this discrepancy can be found in the C, N and O concentrations of the sample neglected in the 1D simulation. If the SDTrimSP-1D simulation includes the elemental depth distribution, as measured with XPS, the resulting sputtering yield is closer to the experimental data, but still too high and the transient effect at very low fluences is not well reproduced. The SDTrimSP-2D simulation in addition also includes the initial surface morphology and all dynamically changes during simulated ion irradiation, which leads to an almost perfect agreement with the experimental data. Both the steady state sputtering yield of 1.9 Fe/Ar as well as the transient effects at very low fluences are very well reproduced.

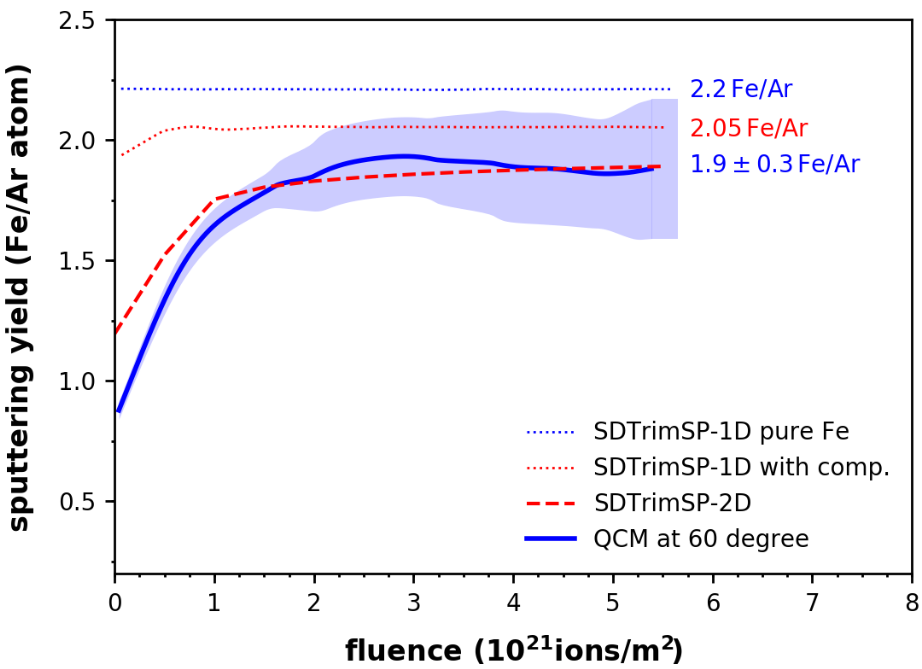


**Figure 5:** Measured sputtering yield for 500 eV Ar ions bombarding an iron film under an angle of incidence of 60°, as a function of the Ar ion fluence (thick blue line). The increase of the sputtering yield at low fluences indicate a sputtering of an oxide layer. The dashed line represent numerical simulations with SDTrimSP-1D and 2D. Taking into account the actual elemental composition of the target improves the 1D-simulation (red dotted line) somewhat. By including the surface morphology in a SDTrimSP-2D simulation (thick red dashed line) the agreement with experimental results can be substantially improved.

In fig. 6 experimental data for the measured and simulated Fe sputtering yields as a function of nominal impact angle are compared for two cases: The green triangles show the situation of the "unirradiated" target. In addition to the full dynamic SDTrimSP-2D results also data obtained with the 1D version of SDTrimSP are compared, assuming a pure and perfectly flat Fe target, as well as including the elemental depth concentration of the sample. Neither the absolute value nor the qualitative characteristic of the angular dependence can be reproduced correctly with the 1D simulation, while agreement with the 2D version is excellent.

After a total fluence of 6.7 x $10^{21}$ Ar/$m^2$, applied under an angle of incidence of 60 degrees, the agreement with SDTimSP-2D as well as SDTrimSP-1D, which includes the elemental depth distribution, is very good. The more pronounced impact angle dependence indicates an ion induced smoothening of the surface, which is confirmed by the AFM measurements (fig. 3).

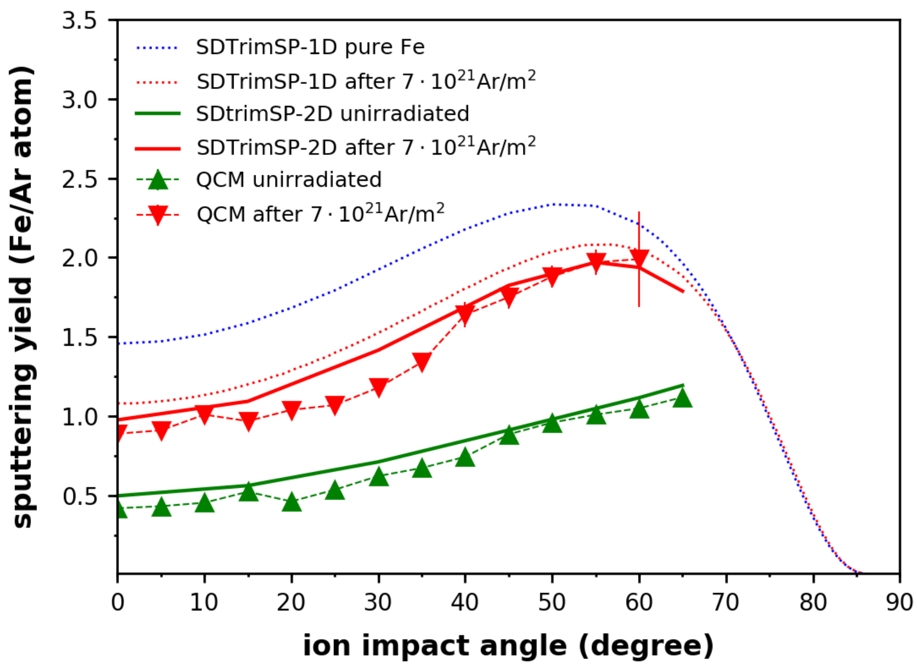


**Figure 6:** The green triangles give the measured Fe sputtering yield as a function of nominal impact angle for the unirradiated target surface. A simulation with SDTrimSP-2D (green curve) which includes both the measured surface roughness (from AFM) and elemental composition (from XPS) fits the experimental data much better than a static 1D simulation with SDTrimSP assuming a flat surface (blue dashed curve). The agreement remains excellent when comparing the experimental data for the Fe film (red inverted triangles) irradiated with a total fluence of 6.7 x $10^{21}$ Ar/$m^2$ with a fully dynamic SDTrimSP-2D simulation starting from the initial situation given in fig. 4a. Here the SDTrimSP-1D simulation, which includes the

elemental depth composition but assumes a flat surface (red dotted line), also reproduces the measurement very well. This indicates a surface smoothening by ion irradiation.

The root mean square (RMS) roughness, evaluated from the AFM measurements, show a decrease from about 5.2 nm (fig. 3a) to 3.5 nm (fig. 3b). This smoothing can much better be quantified by the distribution of the local impact angle θ. This distribution can be evaluated also from the AFM data and a comparison between this distribution of angles before and after irradiation is shown in figure 7.

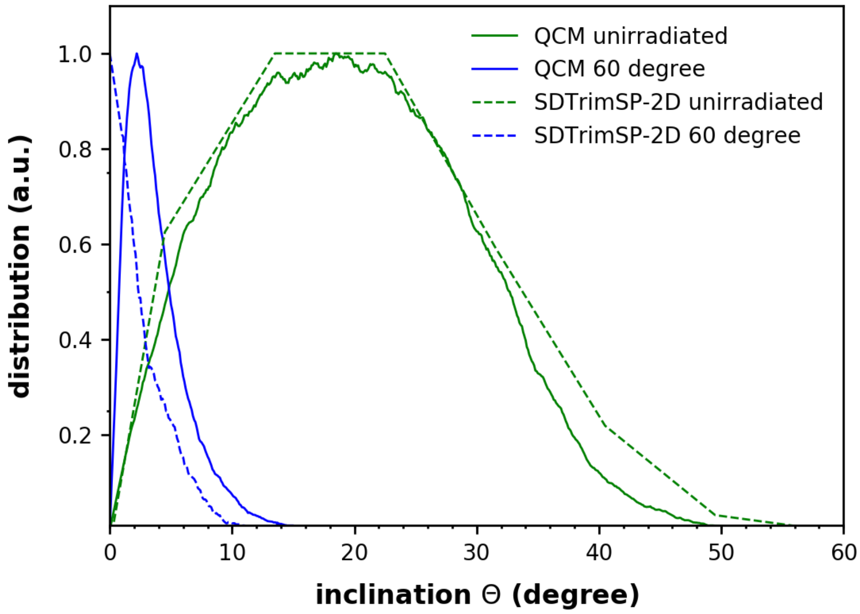


**Figure 7:** The distributions of local impact angle θ (i.e. the angles between the direction of the incident projectile and the local surface normal) as derived from the AFM images in fig. 4, show a shift towards lower angles and a decrease in width after ion-beam irradiation. This can be interpreted as a smoothening of the surface, since an ideally flat sample would correspond to a delta distribution around 0 degrees. The dashed lines show the results of numerical simulations with SDTrimSP-2D.

The distribution of the initial rough surface has a peak at around 20 degrees and is very broad, with a full-with-half-maximum (FWHM) of 28 degrees. The distribution after the irradiation has a peak at 2 degrees and a FWHM of 4 degree. As a perfectly flat surface would be represented by a delta distribution centred at 0 degrees, the surface can be interpreted as much smoother after the ion irradiation. Figure 7 also shows the initial local angular distribution of the unirradiated model surface for SDTrimSP-2D (fig. 4a), which was chosen to match the real surface, evaluated with AFM (fig 3a). After a simulated irradiation by 6.5 x $10^{21}$ Ar/$m^2$ under 60 degrees, the calculated angular distribution narrows to a FWHM of 2.3 degrees and a maximum at 0 degrees. The smoothening is thus confirmed by SDTrimSP-2D, but the remaining small discrepancies between measurement and simulation are probably due to the two dimensional approach. The missing extra dimension reduces possible local impact angles in this dimension, so the local impact angle statistics is shifted to 0 degrees.

## 5. Summary and outlook

Sputtering experiments of Fe samples have been performed, by using a highly sensitive quartz crystal microbalance technique and compared to BCA simulations with the codes SDTrimSP-1D and SDTrimSP-2D. Monoenergetic Ar ions with 500eV/Ar were used to irradiate the samples under an angle of incidence of 60 degrees.

Sputter XPS measurements of the unirradiated samples showed a clear oxide layer on top and an Fe concentration of only 85% with substantial impurities of O, N and C in the bulk.

AFM measurements before and after irradiation with a total fluence of 6.7 x $10^{21}$ Ar/$m^2$ give information about the change in surface morphology, RMS roughness and local impact angle distribution. A clear decrease of the RMS roughness, as well as the width of the local impact angle distribution could be observed. Additionally ripple-like structures, oriented in the direction of the incident ion beam could be seen.

SDTrimSP-1D simulations assuming a pure elemental target and a perfectly flat surface were not able to reproduce the sputtering behaviour. Including the elemental depth composition into SDTrimSP-1D improved the agreement at least for the angular dependent sputtering behaviour of the irradiated sample. Only by considering the actual surface structure and elemental composition in an SDTrimSP-2D simulation, a close agreement between simulation & experiment could be achieved.

While a two dimensional modelling with SDTrimSP-2D is already quite successful, a full 3D, as planned with the new code SDTrimSP-3D, which includes effects like formation of ripple-like structures and to investigate their influence on the sputtering behaviour promises even better results.

## Acknowledgments

*The authors are grateful to Michael Schmid (IAP, TU Wien) for his continued support with the QCM electronics. This work has been carried out within the framework of the EUROfusion Consortium and has received funding from the Euratom research and training programme 2014-2018 under grant agreement No 633053. The views and opinions expressed herein do not necessarily reflect those of the European Commission. Financial support has also been provided by KKKÖ (commission for the coordination of fusion research in Austria at the Austrian Academy of Sciences - ÖAW).*

## References

[1] H. Bolt, V. Barabash, G. Federici, J. Linke, A. Loarte, J. Roth, K. Sato, Plasma facing and high heat flux materials - needs for ITER and beyond, J. Nucl. Mater., 307–311, Part 1 (2002) 43-52.

[2] B. Hapke, Space weathering from Mercury to the asteroid belt, J Geophys Res-Planet, 106 (2001) 10039-10073.

[3] E. Grün, M. Horanyi, Z. Sternovsky, The lunar dust environment, Planet. Space Sci., 59 (2011) 1672-1680.

[4] R. Lindau, A. Moslang, M. Rieth, M. Klimiankou, E. Materna-Morris, A. Alamo, A.A.F. Tavassoli, C. Cayron, A.M. Lancha, P. Fernandez, N. Baluc, R. Schaublin, E. Diegele, G. Filacchioni, J.W. Rensman, B. van der Schaaf, E. Lucon, W. Dietz, Present development status of EUROFER and ODS-EUROFER for application in blanket concepts, Fusion Eng. Des., 75-79 (2005) 989-996.

[5] K. Sugiyama, J. Roth, V.K. Alimov, K. Schmid, M. Balden, S. Elgeti, F. Koch, T. Hoschen, M.J. Baldwin, R.P. Doerner, H. Maier, W. Jacob, Erosion study of Fe-W binary mixed layer prepared as model system for RAFM steel, J. Nucl. Mater., 463 (2015) 272-275.

[6] B.M. Berger, R. Stadlmayr, D. Blöch, E. Gruber, K. Sugiyama, T. Schwarz-Selinger, F. Aumayr, Erosion of Fe-W model system under normal and oblige D ion irradiation, Nuclear Materials and Energy, 2017.

[7] P. Sigmund, Theory of Sputtering. I. Sputtering Yield of Amorphous and Polycrystalline Targets, Phys. Rev., 184 (1969) 383-416.

[8] A. Mutzke, R. Schneider, W. Eckstein, R. Dohmen, SDTrimSP Version 5.00, IPP-Report, Max-Planck-Institut für Plasmaphysik, 2011.
[9] M. Küstner, W. Eckstein, V. Dose, J. Roth, The influence of surface roughness on the angular dependence of the sputter yield, Nucl Instrum Meth B, 145 (1998) 320-331.
[10] M. Küstner, W. Eckstein, E. Hechtl, J. Roth, Angular dependence of the sputtering yield of rough beryllium surfaces, J. Nucl. Mater., 265 (1999) 22-27.
[11] A. Mutzke, R. Schneider, G. Bandelow, SDTrimSP-2D: Simulation of Particles Bombarding on a Two Dimensional Target-Version 2.0, (2013).
[12] A. Mutzke, I. Bizyukov, R. Schneider, J. Davis, Nano-scale modification of 2D surface structures exposed to 6keV carbon ions: Experiment and modeling, Nucl. Instr. Meth. Phys. Res. B, 269 (2011) 582-589.
[13] B.M. Berger, R. Stadlmayr, G. Meisl, M. Čekada, C. Eisenmenger-Sittner, T. Schwarz-Selinger, F. Aumayr, Transient effects during erosion of WN by deuterium ions studied with the quartz crystal microbalance technique, Nucl. Instr. Meth. Phys. Res. B, 382 (2016) 82-85.
[14] G. Hayderer, M. Schmid, P. Varga, H.P. Winter, F. Aumayr, A highly sensitive quartz-crystal microbalance for sputtering investigations in slow ion-surface collisions, Rev. Sci. Instrum., 70 (1999) 3696-3700.
[15] K. Dobes, V. Smejkal, T. Schafer, F. Aumayr, Interaction between seeding gas ions and nitrogen saturated tungsten surfaces, International Journal of Mass Spectrometry, 365 (2014) 64-67.
[16] A. Kallenbach, M. Balden, R. Dux, T. Eich, C. Giroud, A. Huber, G.P. Maddison, M. Mayer, K. McCormick, R. Neu, T.W. Petrie, T. Putterich, J. Rapp, M.L. Reinke, K. Schmid, J. Schweinzer, S. Wolfe, A.U. Team, D.-D. Team, A. Team, J.-E. Contributors, Plasma surface interactions in impurity seeded plasmas, J. Nucl. Mater., 415 (2011) S19-S26.
[17] P. Karmakar, D. Ghose, Ion beam sputtering induced ripple formation in thin metal films, Surf Sci., 554 (2004) L101-L106.
[18] W. Eckstein, The Binary Collision Model, in: Computer Simulation of Ion-Solid Interactions, Springer Berlin Heidelberg, Berlin, Heidelberg, 1991, pp. 4-32.

[19] J.F. Ziegler, M.D. Ziegler, J.P. Biersack, SRIM - The stopping and range of ions in matter (2010), Nucl Instrum Meth B, 268 (2010) 1818-1823.

[20] W. Möller, W. Eckstein, Tridyn - a Trim Simulation Code Including Dynamic Composition Changes, Nucl Instrum Meth B, 2 (1984) 814-818.

[21] W. Möller, W. Eckstein, J.P. Biersack, Tridyn - Binary Collision Simulation of Atomic-Collisions and Dynamic Composition Changes in Solids, Comput. Phys. Commun., 51 (1988) 355-368.

[22] H. Hofsäss, K. Zhang, A. Mutzke, Simulation of ion beam sputtering with SDTrimSP, TRIDYN and SRIM, Applied Surface Science, 310 (2014) 134-141.

[23] I. Bizyukov, A. Mutzke, R. Schneider, J. Davis, Evolution of the 2D surface structure of a silicon pitch grating under argon ion bombardment: Experiment and modeling, Nucl. Instr. Meth. Phys. Res. B, 268 (2010) 2631-2638.